Nucleation and Growth of CdSe on ZnS Quantum Crystallite Seeds, and Vice Versa, in Inverse Micelle Media

A. R. Kortan, R. Hull, R. L. Opila, M. G. Bawendi, M. L. Steigerwald, P. J. Carroll, and L. E. Brus*

Contribution from AT&T Bell Laboratories, Murray Hill, New Jersey 07974.
Received June 20, 1989

Abstract: Composite semiconductor crystallites involving CdSe grown on an ZnS seed,and vice versa, have been synthesized and "capped" with organic ligands in inverse micelle solutions. These composite particles, as well as capped seed crystallites of CdSe and ZnS, are isolated, purified, and characterized for relative atomic composition, structure, and electronic properties. The Debye X-ray scattering equation, when solved for these layered particles, shows that powder X-ray scattering is insensitive to a small foreign inclusion. A simple theoretical model for the LUMO and HOMO of layered crystallites shows that a small (<15-Å diameter) interior foreign seed causes only small shifts of the lowest excited state, to either higher or lower energies. The capped CdSe seed and the capped CdSe portion of the layered particle grown on a ZnSe seed undergo low-temperature (169 °C) annealing to give near-single-crystal X-ray scattering. However, CdSe annealing is blocked by a surface ZnS layer which is ca. 4 Å thick. While growth to make composite particles does occur, neither particle shows evidence for epitaxial growth.

Semiconductor quantum crystallites (20–60-Å diameter) have incomplete band structure development, even though the bulk unit cell is present. Their optical and electronic properties are size dependent, and within the past 5 years synthetic procedures have been developed to prepare and stabilize uniform crystallites.[1,2] Inverse micelle solutions provide a medium for synthesis of stable, size-selected semiconductor colloids.[3] CdSe crystallites in inverse micelles do not fuse with one another because of the surfactant, yet they can grow larger if either ionic or organometallic sources of Cd and Se atoms are added.[4] This surface reactivity was exploited in an organic "capping" reaction:

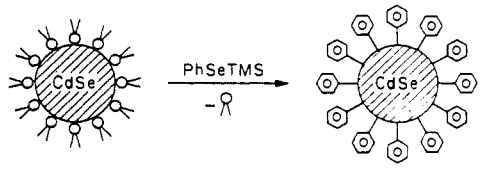

(1)

♀ = SURFACTANT MOLECULE

Various organic groups (here phenyl) were bonded to the surface, passivating the surface and allowing the (CdSe)cap clusters to be isolated in pure powder form.[4] Their electronic hole-burning,[5] resonance Raman,[6] higher-pressure optical,[7] and NMR spectra[8] have been reported.

We now explore possible growth of one material on a seed of another. As shown in a later section, the electronic structure of such layered crystallites promises to be far more interesting and diverse than that of single-material crystallites. We utilize CdSe and ZnS, which both exhibit tetrahedrally coordinated structures and direct band gaps. CdSe has a band gap of 1.7 eV and a cubic lattice constant of 6.08 Å, while ZnS has a band gap of 3.2 eV and a lattice constant of 5.40 Å. This difference in lattice constants implies that the solid-state Cd–Se bond length is 13% longer than the Zn–S bond length. We start with a bare, micelle-encapsulated seed of one material and attempt to grow a capped outer layer, e.g. $(ZnS)_1(CdSe)_4Ph$. This notation implies that a ZnS interior seed is (ideally) surrounded by a concentric shell of CdSe. The entire particle is capped with phenyl groups. We choose a nominal four-to-one stoichiometry so that the outer layer would be roughly as thick as the inner seed if uniform growth occurred. These capped clusters are isolated, purified, and physically characterized.

It is known from aqueous colloidal experiments that inorganic ions can chemisorb on semiconductor quantum crystallites and can have marked effects on luminescence.[9] In our experiment the basic question is whether a foreign monolayer can continue to grow into a thick outer layer or whether separate nucleation of the added semiconductor regents will occur. We utilize synthetic procedures where it is already established that added Cd and Se reagents grow onto a CdSe seed, making a larger crystallite.[4] This example is a trivial case of epitaxial growth. An adsorbed CdSe layer on a ZnS seed, however, would be expected to be strained because ZnS has a shorter bond length. Further, added Cd and Se reagents might nucleate separately rather than grow on this strained seed. On the other hand, the highly curved interface might naturally relieve much of the expected strain.

Layered, planar semiconductor growth has been extensively studied.[10] While little is known structurally about such possible concentric inorganic composite crystallites, several studies indicate promising electrical behavior for CdS crystallites with ZnS fragments on the surface, and/or coprecipitated ZnS–CdS particles.[11-13] Strongly luminescencing CdS particles with a $Cd(OH)_2$ monolayer on the surface,[9c] and near monolayer WO_3 deposited on large silica particles,[14] have been made and optically characterized. Photoinitiated electron transfer between touching colloidal TiO_2 and CdS particles, made by mixing of colloids, has been

(1) Steigerwald, M. L.; Brus, L. E. *Annu. Rev. Mater. Sci.* **1989**, *19*, 471.
(2) Henglein, A. *Top. Curr. Chem.* **1988**, *143*, 113.
(3) (a) Meyer, M.; Walberg, C.; Kurihara, K.; Fendler, J. H. *J. Chem. Soc., Chem. Commun.* **1984**, 90. (b) Lianos, P.; Thomas, J. K. *Chem. Phys. Lett.* **1986**, *125*, 299. (c) Dannhauser, T.; O'Neil, M.; Johansson, K.; Witten, D.; McLendon, G. *J. Phys. Chem.* **1986**, *90*, 6074. (d) Petit, C.; Pileni, M. P. *J. Phys. Chem.* **1988**, *92*, 2282.
(4) Steigerwald, M. L.; Alivisatos, A. P.; Gibson, J. M.; Harris, T. D.; Kortan, R.; Muller, A. J.; Thayer, A. M.; Duncan, T. M.; Douglass, D. C.; Brus, L. E. *J. Am. Chem. Soc.* **1988**, *110*, 3046.
(5) Alivisatos, A. P.; Harris, A. L.; Levinos, N. J.; Steigerwald, M. L.; Brus, L. E. *J. Chem. Phys.* **1988**, *89*, 4001.
(6) Alivisatos, A. P.; Harris, T. D.; Carroll, P. J.; Steigerwald, M. L.; Brus, L. E. *J. Chem. Phys.* **1988**, *90*, 3463.
(7) Alivisatos, A. P.; Harris, T. D.; Brus, L. E.; Jayaraman, A. *J. Chem. Phys* **1988**, *89*, 5979.
(8) Thayer, A. M.; Steigerwald, M. L.; Duncan, T. M.; Douglass, D. C. *Phys. Rev. Lett.* **1988**, *60*, 2673.
(9) (a) Henglein, A. *Ber. Bunsenges. Phys. Chem.* **1982**, *86*, 301. (b) Rossetti, R.; Brus, L. *J. Phys. Chem.* **1982**, *86*, 4470. (c) Spanhe, L.; Hasse, H.; Weller, H.; Henglein, A. *J. Am. Chem. Soc.* **1987**, *109*, 5649.
(10) Ploog, K. *Angew. Chem., Int. Ed. Engl.* **1988**, *27*, 593.
(11) Ueno, A.; Kakuta, N.; Park, K. H.; Finlayson, M. F.; Bard, A. J.; Campion, A.; Fox, M. A.; Webber, S. E.; White, J. M. *J. Phys. Chem.* **1985**, *89*, 3828.
(12) Mau, A. W. H.; Huang, C. B.; Kakuta, N.; Bard, A. J.; Campion, A. J.; Fox, M. A.; White, J. M.; Webber, J. M. *J. Am. Chem. Soc.* **1984**, *106*, 6537.
(13) Youn, H. C.; Baral, S.; Fendler, J. H. *J. Phys. Chem.* **1988**, *92*, 6320.
(14) Leland, J. K.; Bard, A. J. *Chem. Phys. Lett.* **1987**, *139*, 453.

0002-7863/90/1512-1327$02.50/0

observed spectroscopically.[15] Fluorescence studies apparently involving very small Ag_2S deposits on CdS particles have been reported.[16]

In this paper we stress the electronic structure and physical characterization of such putative layered structures. We investigate in detail the X-ray powder patterns and electronic (i.e., optical) properties of capped, isolated, layered particles. Section I describes synthesis and optical characterization during growth. Section II describes compositional characterization of seeds and composite crystallites, and Section III describes structural characterization. Section IV outlines a theory of electronic structure in layered particles and compares this theory to our observations. Section V discusses and summarizes our results.

I. Synthesis and Optical Characterization during Growth

We have described in detail the synthesis and capping of CdSe crystallites in AOT (bis(2-ethylhexyl)sulfosuccinate, disodium salt) micellar media.[4] Standard inert atmosphere procedures and deoxygenated solvents were used throughout. Thiophenol-capped ZnS particles, and CdSe particles with two different caps, were prepared in procedure A. Procedure B describes the preparation of the two-layered, capped composite particles. In the following, a micellar solution consists of a heptane solution of AOT (0.12 M) and water (0.96 M).

Procedure A1, (ZnS)Ph: A sulfide solution was made by dissolving 150 μmol of Na_2S in 40 mL micellar solution. This solution was injected with stirring into 255 mL of micellar solution containing 160 μL of 1 M aqueous $Zn(ClO_4)_2$. To this was added, dropwise, 70 μL of 1 M aqueous $Zn(ClO_4)_2$. Finally thiophenol (70 μL in 10 mL of heptane) was injected with stirring, immediately followed by ca. 1 mL of pyridine. The solution became turbid at this point. A white powder obtained by filtering on a fine frit was washed three times with petroleum ether.

Procedure A2, (CdSe)Ph and (CdSe)ZnSPh: (CdSe)Ph particles were capped with Cd ions and Se–phenyl groups as previously described.[4] As a control experiment for procedure B2, we also synthesized (CdSe)-ZnSPh, CdSe particles capped with the Zn ion and the thiophenol group: 14 μL of $Se(trimethylsilyl)_2$ in 15 mL of heptane was injected into 255 mL of micellar solution containing 80 μL of 1 M aqueous $Cd(ClO_4)_2$. Next 80 μL of 1 M aqueous $Zn(ClO_4)_2$ was added dropwise, followed by injection of 100 μL of thiophenol in 15 mL of heptane. Then 1 mL of pyridine was added, and turbidity developed. A dark red powder was filtered and washed as in procedure A1.

Procedure B1, $(ZnS)_1(CdSe)_4Ph$: Twenty milliliters of the sulfide solution described in A1 was injected into 255 mL of micellar solution containing 80 μL of 1 M aqueous $Zn(ClO_4)_2$, making a ZnS colloid. A separate micellar solution containing 240 μL of 1 M aqueous $Cd(ClO_4)_2$ was prepared. A third solution contained 42 μL of $Se(trimethylsilyl)_2$ in 40 mL of heptane. The Cd and Se solutions were injected alternately, in steps of $^1/_{20}$ of their total volumes, into the stirred ZnS colloid. During the injection, the solution developed intense orange-red color. $Cd(ClO_4)_2$ (80 μL of 1 M aqueous) was added dropwise. Phenyl(trimethylsilyl)-selenide (75 μL in 10 mL of heptane) was injected, followed immediately by approximately 1 mL of pyridine. A dark red solid precipitated, leaving a colorless supernatant. The solid was filtered and washed.

Procedure B2: $(CdSe)_1(ZnS)_4Ph$: This procedure is similar to B1, with an interchange of the Cd and Se reagents with those of Zn and S. In the second layer growth stage, both Zn^{2+} and S^{2-} were added (in 20 equal steps) as micellar solutions. Thiophenol substitutes for phenyl-(trimethylsilyl)selenide in the capping stage. Orange-red color developed during the CdSe stage, and there is no further color change during the ZnS stage.

Optical absorption and luminescence spectra, taken by removal of small aliquots between steps of the synthesis, provide insight into these layered growth processes. In general, absorption spectra probe the crystallite internal molecular orbitals and provide information concerning size and particle composition.[17] Luminescence is experimentally sensitive to surface structure, and it normally comes from recombination of electrons and holes in surface states.[18]

In reaction B2, the CdSe seed absorption spectrum in the micelle before ZnS growth shows a broad exciton peak near 500 nm in Figure 1A. This spectrum does not change during ZnS growth and capping, as expected if CdSe is covered by a layer of a much larger band gap

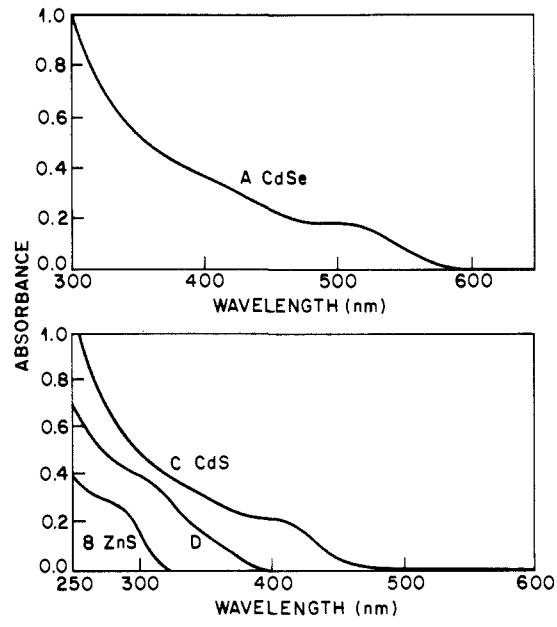

Figure 1. (A) Absorbance (1 cm) of a bare CdSe seed in micellar solution in procedure B2. (B) Absorbance of a bare ZnS seed in procedure B1. (C) Absorbance of a bare CdS seed made by substitution of the Cd ion for the Zn ion in procedure B1. (D) Observed after reaction of a ZnS seed (B) with added Cd ion, as described in the text.

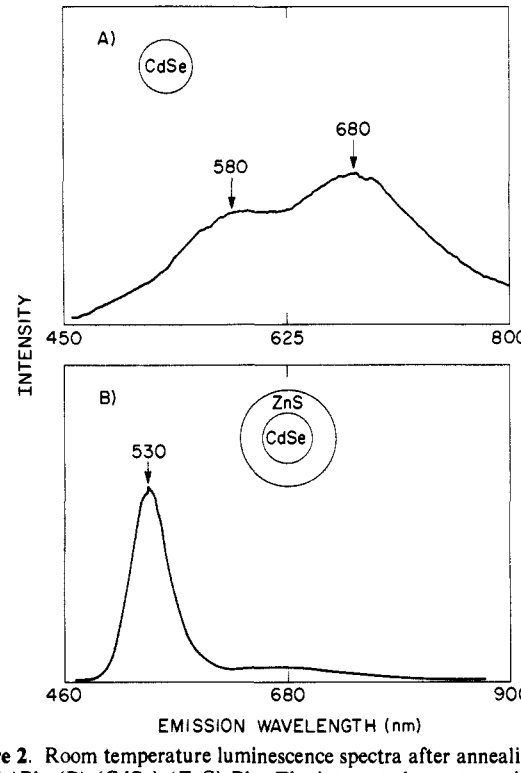

Figure 2. Room temperature luminescence spectra after annealing: (A) (CdSe)Ph, (B) $(CdSe)_1(ZnS)_4Ph$. The integrated quantum yield in B is more than an order of magnitude higher than in A.

material. This result also demonstrates that alloying or surface etching of CdSe by ZnS does not occur.

Luminescence spectra clearly indicate that some surface modification, which we attribute to partial growth of ZnS on CdSe, occurs. The initial CdSe seed shows extremely weak, broad visible emission similar to that in Figure 2A. This luminescence is due to recombination of carriers in deep surface traps.[18] However, after ZnS growth, the quantum yield significantly increases, and the spectrum shifts blue to a narrow band near the exciton absorption, as in Figure 2B. As in the earlier CdS experiments with $Cd(OH)_2$ monolayers,[9c] this observation indicates some ZnS growth to fill the deep surface traps. If ZnS separately nucleated entirely, then bare CdSe particles would be capped with Zn ions and thiophenol as in procedure A2 to make (CdSe)ZnSPh. However, the

(15) Spanhel, L.; Henglein, A.; Weller, H. *Ber. Bunsenges, Phys. Chem.* **1987**, *91*, 1359.
(16) Spanhel, L.; Weller, H.; Fojtik, A.; Henglein, A. *Ber. Bunsenges, Phys. Chem.* **1987**, *91*, 88.
(17) Brus, L. E. *New. J. Chem. (Fr.)* **1987**, *11*, 23.
(18) Chestnoy, N.; Harris, T. D.; Hull, R.; Brus, L. E. *J. Phys. Chem.* **1986**, *90*, 3393.

Table I. Observed Elemental Ratios in EDS and Auger Data[a]

EDS (relative stoichiometries)			Auger (relative intensities)			
Cd/Se	Cd/Zn	Zn/S	Cd/Se	Cd/Zn	Zn/S	material
		0.95			0.45	(ZnS)Ph
0.8			3.5			(CdSe)Ph
0.8	8.0	0.75	4.2	7	1.1	$(ZnS)_1(CdSe)_4Ph$
0.9	1.0	0.8	4.3	1.7	0.46	$(CdSe)_1(ZnS)_4Ph$

[a] EDS data are absolute stoichiometry ratios. Auger data are not corrected for elemental sensitivity factors and cannot be compared with EDS data. Auger ratios can be compared among themselves. The ratios have a reproducibility of about 20%.

luminescence from (CdSe)ZnSPh is extremely weak broad trap emission both before and after capping with Zn ion and thiophenol. Upon redissolving in pyridine, both (CdSe)Ph and (CdSe)ZnSPh show weak broad trap emission, while $(CdSe)_1(ZnS)_4Ph$ continues to show strong edge emission.

In the B1 $(ZnS)_1(CdSe)_4Ph$ reaction, the initial ZnS bare seed has an exciton bump near 280 nm as in Figure 1B, indicating roughly 25 Å diameter particles.[19] After CdSe growth, significant absorption extends, without resolved features, out to 550 nm. As CdS has a lower solubility product than ZnS, Cd ions might displace ("etch") Zn ions in the first stages of the growth process (eq 2). In several control experiments, we

$$Cd^{2+} + ZnS \rightarrow Zn^{2+} + CdS \quad (2)$$

added the Cd^{2+} ion to bare ZnS seeds in the micelle. There is a significant change in the ZnS spectrum as shown in Figure 1B. The spectrum evolves toward that of CdS; this evolution stops when the added Cd ion is about 50% of the initial Zn. Under these experimental conditions, Cd appears to either (1) displace surface Zn or (2) adsorb on surface S^{2-} ions, to make a particle with a CdS-like surface. If displacement occurs as in reaction 2, then the ZnS core in the B1 reaction may be smaller than the initial 25-Å size. There may also be a compositionally graded interface between CdSe and ZnS, this being a combination of effects (1) and (2).

In all these procedures, the resulting powders dissolve in pyridine and 4-alkylpyridines. For EDS (energy dispersive X-ray spectra) and Auger experiments, an aliquot of each pyridine solution is evaporated on a clean Si wafer, leaving a sparse residue. The residue is excited by 10-keV electrons for Auger and 20-keV electrons for EDS measurements in a Perkin-Elmer high-vacuum system. EDS intensities are calibrated by examination of commercial powder bulk CdSe and ZnS samples. The bulk samples are assumed to have one-to-one stoichiometry. Powders are pressed at several kbar into pellets for x-ray scattering measurements. Annealing experiments are conducted in refluxing solvents (3 mg of powder/mL of solvent) under argon.

II. X-ray Fluorescence (EDS) and Auger Spectroscopy

The capped seeds and the capped composite particles are characterized for Se, S, Cd, and Zn relative composition (Table I). EDS samples composition to a depth of about 1 μm while Auger is a surface-sensitive technique. Approximate calibration curves indicate that the Zn and Se Auger transitions we observe, at 994 and 1315 eV, respectively, should have escape depths on the order of 30 Å. The S and Cd transitions at 152 and 375 eV should have escape depths of less than 10 Å. Note that the EDS ratios are absolute stoichiometric ratios in Table I, while Auger ratios are relative signal intensity ratios. They cannot be directly compared. Changes in Auger ratios can only be compared from one sample to the next.

The Auger and EDS ratios for ca. 25 Å diameter (ZnS)Ph particles are very close to those of authentic bulk powder ZnS. This result is consistent with stoichiometric crystallites. In powders that have been repeatedly washed with petroleum ether before redissolving in 4-ethylpyridine for refluxing, The EDS and Auger data also show negligible Cl peak. This observation indicates that the (ZnS)Ph powder has no counterion ClO_4^-, which is present in the inverse micelle reaction medium. The CdSe particles are Se rich, with stoichiometry Cd/Se typically 0.8. As the particle interior is crystalline, it must be that the surfaces naturally form Se rich. These powders also show negligible presence of the counterions Na^+ and ClO_4^-, and no S signal from possible AOT contamination.

The EDS ratios for $(ZnS)_1(CdSe)_4$cap are consistent with etching of the initial 25-Å ZnS seed as in reaction 2. In the capped powder, the Cd/Zn ratio is experimentally 8 instead of 4, and the Zn/S ratio is below 1. To explain this result, displacement must occur, and the etched ions must remain in solution after capping.

In the $(CdSe)_1(ZnS)_4Ph$ case, the measured EDS Cd/Zn ratio is 1.0 instead of 0.25. As discussed, optical spectra indicate that the CdSe seeds are not etched. We tentatively propose that the Zn and S reagents partially grow on the CdSe seeds (as required by luminescence data) and also partially separately nucleate to form very small ZnS particles. In this hypothesis the very small ZnS particles remain in solution after capping. In this regard, note that (ZnS)Ph particles in procedure A1 are recovered only in low yield from micelle solution when filtering with a fine frit and appear to be more soluble than the 40-Å (CdSe)cap particles in procedure A2, which are recovered in near quantitative yield after capping.

In (CdSe)ZnSPh where Zn ion and thiophenol, followed by pyridine, are used to cap CdSe, the measured Cd/Zn ratio is 8. There is less than a monolayer of Zn ion adsorbed on CdSe, and thus the Zn plus S–phenyl capping reaction on CdSe does not appear to work well. The solution only becomes turbid after pyridine is added, which suggests that the CdSe particles are capped principally with pyridine coordinated to surface Cd ions. The fact that the particles redissolve in pyridine without aggregation indicates the particles are capped.

In the table, changes in Auger intensity ratios approximately mirror changes in EDS ratios, when comparing samples. An exception is the Auger Zn/S ratio for (ZnS)Ph compared with the $(ZnS)_1(CdSe)_4Ph$ composite particle. If the ZnS is inside the CdSe, the S Auger electrons would be expected to be attenuated more than the Zn Auger electrons. Consistent with this, the Zn/S Auger ratio is high for the composite particle. However, the Zn and S Auger signals are not as weak as might be expected for only interior ZnS seeds. This result suggests some capped ZnS is present, either as separately nucleated particles or as part of a composite particle with incomplete CdSe coating. Similarly, the Cd/Zn Auger ratio for $(ZnS)_1(CdSe)_4Ph$ is probably too low for this reason.

III. Structural Characterization

(1) (CdSe)Ph and Annealing of the Crystal Structure. While the EDS and Auger data reveal elemental composition, the X-ray diffraction and transmission electron microscopy (TEM) data reveal structure. Figure 3 shows the powder X-ray pattern of (CdSe)Ph as well as the calculated powder pattern for a single crystal of zinc blende 37 Å diameter for Mo Kα radiation.[20] The Figure 3A pattern of the (as recovered) powder is markedly broader than the calculated powder pattern. We found that heating these (CdSe)Ph particles to reflux in 4-ethylpyridine (169 °C) for 45 min narrows the lines as in Figure 3B, without changing the 35–40-Å particle size as measured in direct TEM imaging. After such "annealing", the major ⟨111⟩ peak at $2\theta \simeq 12°$ has a width that agrees (within 20%) with that expected for 37 Å finite size broadening (Figure 3C). This result indicates that the annealed particles are close to being internally perfectly crystalline, with a bond length the same as in the bulk crystal.[20] The as-prepared crystallites are essentially polycrystalline. However, the initial structural defects are substantially removed at 169 °C, a temperature far lower than would be required for the annealing of the bulk materal, which melts at 1512 K.

(19) Rossetti, R.; Hull, R.; Gibson, J. M.; Brus, L. E. *J. Chem. Phys.* **1985**, *82*, 552.

(20) Numerically calculated from the Debye powder pattern scattering function (Guinier, A. *X-Ray Diffracton*; W. H. Freeman: San Francisco, 1963), eq 2.54) using Cd and Sd atomic scattering factors from D. T. Cromer and J. B. Mann: *Acta Crystallogr.* **1968**, *A24*, 321. The bulk zinc-blende crystal structure is assumed. Better agreement with the annealed (CdSe)Ph powder pattern at larger scattering angles can be achieved with inclusion of thermal broadening and growth alternations between zinc-blende and wurtzite along the 111 direction. (Bawendi, M. G., et al. *J. Chem. Phys.* **1989**, *91*, 7282.)

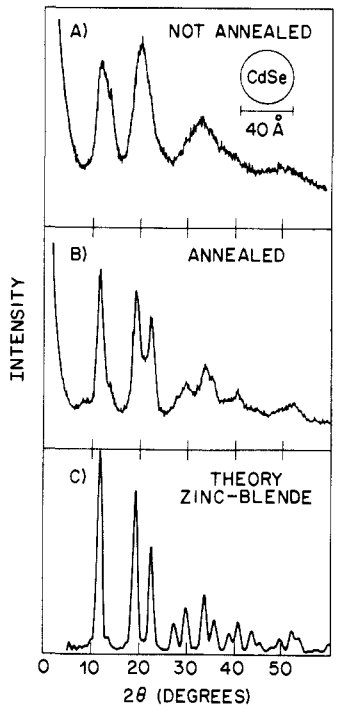

Figure 3. X-ray powder pattern of (CdSe)Ph material before and after annealing. Panel C shows the powder pattern calculated from the Debye equation for a 37 Å diameter spherical crystallite, as described in ref 20. In C the line widths reflect the finite size of the crystallite.

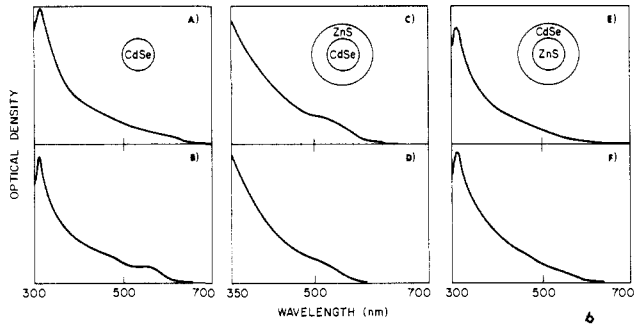

Figure 4. Room temperature optical absorption spectra in 4-ethylpyridine, both before (upper trace) and after (lower trace) annealing: (A, B) (CdSe)Ph, (C, D) $(CdSe)_1(ZnS)_4Ph$, (E, F) $(ZnS)_1(CdSe)_4Ph$.

Parts A and B of Figure 4 show the optical spectra of 40 Å diameter (CdSe)Ph crystallites before and after annealing. Optical hole-burning experiments have shown that the broad peak in the 550-nm region is the 1S–1S lowest excited state.[5] The transition is inhomogeneously broadened; that is, one crystallite is different from another due to size, shape, the presence of defects, and/or differing surface structures. These differences cause each crystallite to absorb at a slightly different wavelength. The 1S–1S transition in annealed samples is significantly sharper. This sharpening is the optical analogue of the X-ray powder pattern sharpening. The size and shape variation of the crystallites are unchanged by annealing under TEM analysis.

(2) (ZnS)Ph. Figure 5 shows the powder X-ray pattern of capped ZnS seeds after refluxing in 4-ethylpyridine at 169 °C. The near 280 nm exciton position observed in micellar solution indicates that the ZnS diameter is about 25 Å, from prior TEM measurements.[19] The calculated X-ray pattern for a 25-Å particle shows considerably more structure than is actually observed. This observation is consistent with either of two interpretations: (1) the annealed particles are disordered, like the (CdSe)Ph particles before annealing (bulk ZnS melts at a higher temperature than bulk CdSe, and therefore should anneal at a higher temperature) or (2) the particles all have a reconstructed structure slightly different than the bulk, with a range of Zn–S bond lengths. The (111) diffraction peak is centered at a slightly larger angle than

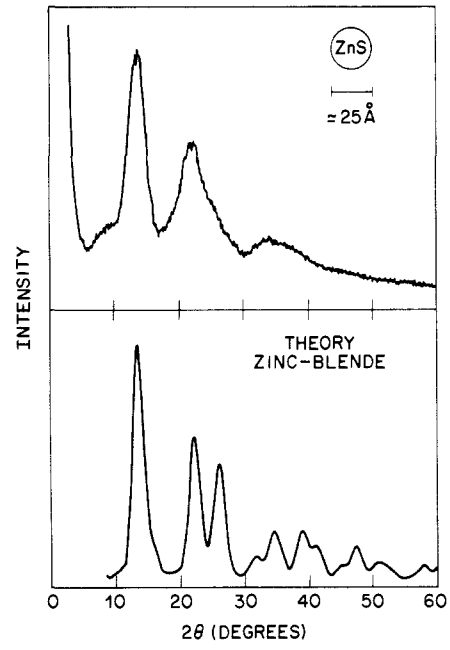

Figure 5. X-ray powder pattern of (ZnS)Ph materal after annealing. The lower panel shows the calculated pattern for 25 Å diameter ZnS zinc-blende crystallite.

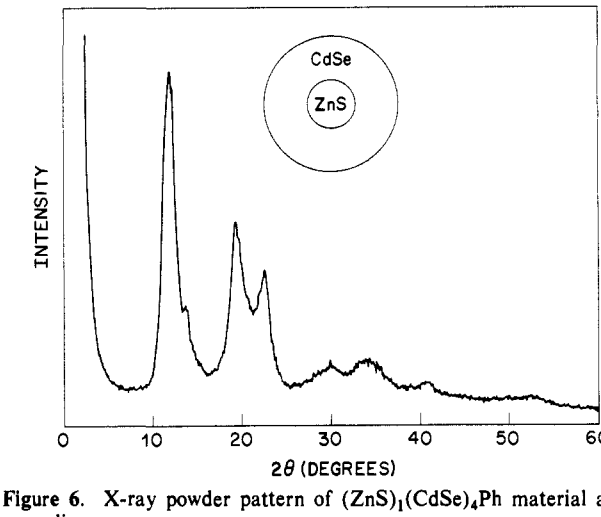

Figure 6. X-ray powder pattern of $(ZnS)_1(CdSe)_4Ph$ material after annealing.

expected for bulk ZnS, suggesting that the average bond length in the particle is ca. 3% shorter than in the bulk crystal.

(3) $(ZnS)_1(CdSe)_4Ph$. In the case of CdSe growth on a ZnS seed (followed by annealing) in Figure 6, we have a remarkable result: the powder X-ray pattern is essentially the same as for a pure capped *annealed* CdSe crystallite (Figure 3). Recall that the EDS Cd/Zn stoichiometry ratio is ca. 8 for these annealed particles. In addition the X-ray scattering factors are higher for Cd and Se than for Zn and S. Thus, the X-ray pattern is dominated by CdSe scattering in the composite particle. The outer CdSe material appears to adapt to its own crystal structure, despite the fact that a tiny ZnS fragment is incorporated. The initially polycrystalline CdSe lattice anneals coherently on the (etched) ZnS seed.

One might propose that we in fact observe separately nucleated (CdSe)Ph particles that contain no Zn or S. The unannealed optical absorption spectrum in Figure 4E is somewhat similar to that of similarly size (CdSe)Ph in Figure 4A. However, both the 1S–1S exciton absorption feature and the luminescence are different than those of genuine (CdSe)cap particles after having been annealed. First, while the X-ray spectra do sharpen upon annealing, the 1S–1S exciton bump is present neither before nor after annealing (Figure 4, E and F), in contrast to that of genuine

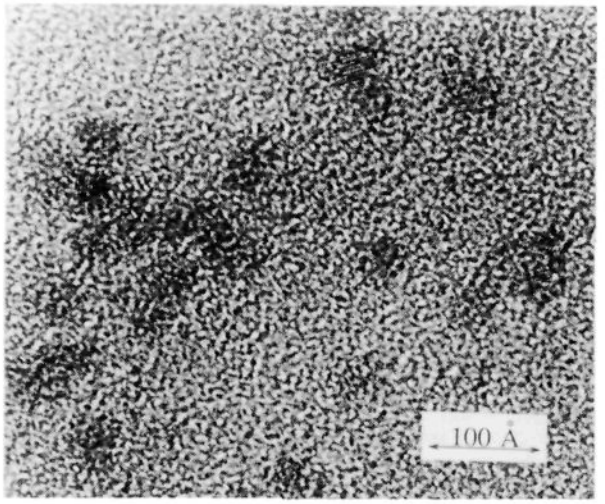

Figure 7. Bright field transmission electron micrograph of $(ZnS)_1(CdSe)_4Ph$ particles. Particles showing lattice images have ⟨111⟩ axes in the plane of the photograph.

(CdSe)Ph (Figure 4, A and B). (We model this result in section IV on electronic properties of layered particles; basically the tiny foreign inclusion introduces additional broadening due to the size, location, and composition of tiny inclusion.) Second, the luminescence of annealed $(ZnS)_1(CdSe)_4Ph$ is far weaker than that of genuine (CdSe)Ph in Figure 2A. The etched ZnS inclusion appears to introduce deep interior traps where the electron and hole nonradiatively recombine.

Direct TEM observation of annealed $(ZnS)_1(CdSe)_4Ph$ (Figure 7) shows an average diameter of 45 Å with a standard deviation of 13%. Many particles show partially resolved zinc-blende ⟨111⟩ lattice planes, whose spacing is consistent with CdSe. The experimental 8/1 Cd/Zn stoichiometry ratio is consistent with a ZnS core of approximately 18-Å diameter, assuming the concentric shell model. It is possible that a fraction of the recovered ZnS in this sample is separately nucleated capped ZnS particles, as suggested by Auger intensity ratios. In this case the average ZnS core would be smaller than 18 Å.

The composite is a CdSe single crystal with an unobserved foreign inclusion. How can the X-ray spectra be essentially the same as those of (CdSe)Ph particles? We model such crystallites as having small interior holes. The top panel of Figure 8 shows the powder X-ray pattern calculated from the Debye formula, for a 45-Å CdSe single crystal with a 18-Å hole at the center. The bottom trace shows the case of a 36-Å hole. In these shell crystals, each Bragg line develops a broad base around the sharp central line. The broad bases effectively add to the background continuum already present due to thermal diffuse scattering, surface reconstruction, and growth faults, as already discussed for normal CdSe crystallites in Figure 3. We conclude from comparison of Figure 8 and Figure 3 that, at the present level of experimental crystalline quality, the X-ray pattern by itself *does not indicate* if there is a small missing volume (defined in terms of the percentage of missing atoms) inside the single crystal. Our composite crystallites have *at most* 18-Å ZnS cores, calculated from the experimental EDS ratios. X-ray scattering from these cores should simply add to that of the coherent CdSe shells. We calculated that the ZnS ⟨111⟩ peak integrated area should be a factor of 27 less than the CdSe peak because of the scattering factors and the atomic ratios. Thus the ZnS scattering will not be resolved in the composite X-ray scattering. This result is consistent with the optical spectrum which, as discussed in section IV, implies that ZnS inclusions are smaller than roughly 15 Å.

(4) $(CdSe)_1(ZnS)_4Ph$. In the case of ZnS growth on a CdSe seed, the annealed material powder X-ray pattern is broad (Figure 9). The strong ⟨111⟩ peak, which is most characteristic of the nearest-neighbor bond length, is shifted to smaller angle than in annealed ZnS, and to larger angle than in annealed CdSe. The

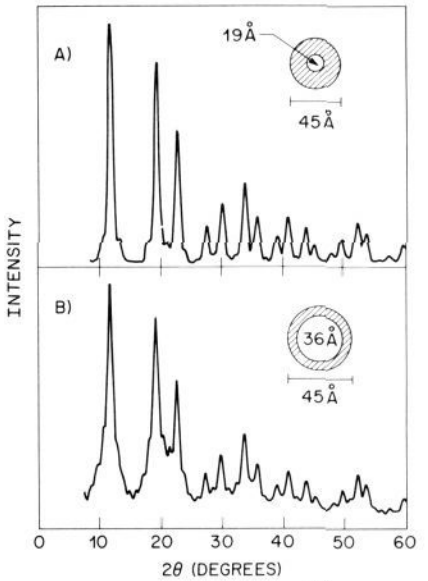

Figure 8. Calculated powder patterns for a 45 Å diameter CdSe crystallite with an 19 Å diameter hole in the center (top panel) and a 36 Å hole in the center (bottom panel).

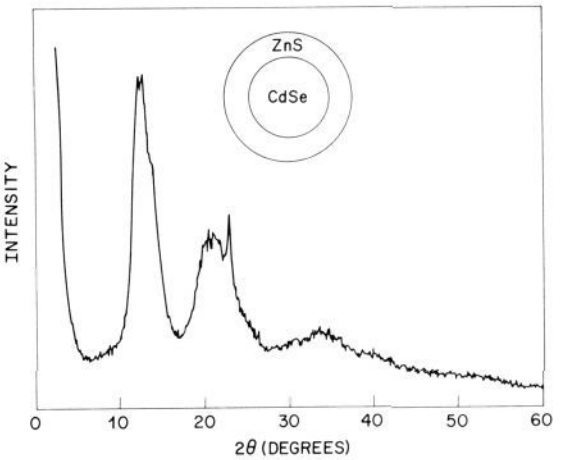

Figure 9. X-ray powder pattern of $(CdSe)_1(ZnS)_4Ph$ material after annealing.

peak is too broad for the composite to be characterized by a single intermediate unit cell size, valid over the entire composite crystallite. Recall that the EDS Cd/Zn stoichiometry for this composite is 1/1, so that both the ZnS and CdSe components may contribute to the X-ray. We cannot fit this peak as a sum of the annealed CdSe and annealed ZnS spectra. The peak width and position are close to those of *unannealed* CdSe. The composite peaks are at slightly larger angle, and probably have some contribution from ZnS fragments, but absence of sharp ZnS lines indicates that the thin ZnS surface layer is not coherently crystalline around the composite particle.

These X-ray scattering results indicate that annealing of the CdSe core does not occur if the surface is treated with ZnS. The initial CdSe exciton peak indicates that the CdSe seed has a diameter in the 30–35-Å range. The 1/1 EDS stoichiometry in the composite particle indicates that the idealized outer ZnS layer is at most 4 Å thick. The annealed diameter of the composite particle is ca. 40 Å, consistent with these estimates, with few ⟨111⟩ lattice planes being visible.

The inability of these particles to anneal, in contrast to (CdSe)Ph particles, is confirmed in the optical spectra. The exciton bump of the annealed material (Figure 4D) does not narrow or shift, with respect to that of the unannealed material (Figure 4C). This result also indicates that extensive alloying does not occur in 169 °C annealing.

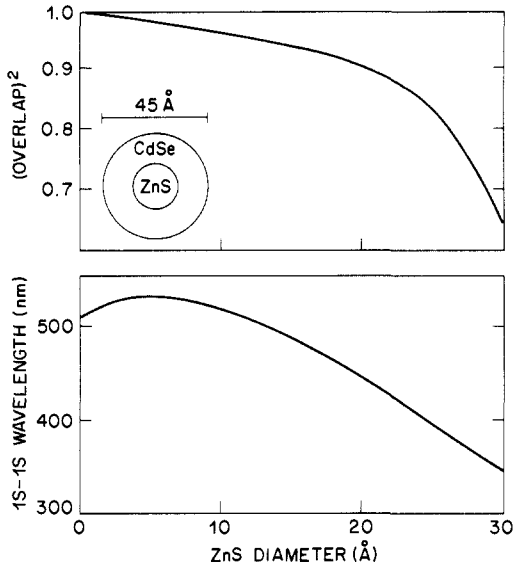

Figure 10. Calculated properties of a 45 Å diameter CdSe crystallite with an internal ZnS seed at the center, as a function of ZnS diameter. Lower panel: optical absorption wavelength of lowest excited state. Upper panel: square of electron-hole overlap integral for this state.

(CdSe)ZnSPh particles, partially capped with Zn ion and S-phenyl, tend to precipitate during refluxing in 4-ethylpyridine, indicating that they are weakly capped. The optical spectrum shows a complete loss of the exciton bump, and the diffraction pattern shows the crystal structure has annealed, after refluxing. These results again confirm that (CdSe)ZnSPh particles behave differently than $(CdSe)_1(ZnS)_4Ph$ particles suggesting that, in the case of $(CdSe)_1(ZnS)_4Ph$, the surface is entirely coated with ZnS that thereby inhibits annealing.

IV. Electronic Structure of Layered Crystallites

In order to model the optical spectra of a CdSe crystallite with a small inclusion of ZnS, we solve Schrödinger's equation for an ideal, layered, spherical crystallite, using the same assumptions and approximations as previously used for single materials.[21] With an epitaxial interface, the effect of the layering is to introduce a step function into the Hamiltonian. The step is the difference in the band edge energies between ZnS and CdSe. There is a different step for both valence and conduction bands. Effective masses are parameters that represent electron delocalization; they vary with material and with band. In the calculation there are four different effective masses, one for each band and each material. The shielded Coulomb interaction is included in first-order perturbation theory. There are no adjustable parameters as the effective masses and band offsets are known bulk properties of CdSe and ZnS.

In Figure 10 we show the energy and electron-hole overlap integral for the lowest excited "1S-1S" state, for a ZnS/CdSe sphere of diameter 45 Å, as a function of the diameter of the inner ZnS seed. The overlap integral determines the intensity of the lowest transition. The valence and conduction band energy offsets are such that both electron and hole are more stable in CdSe than in ZnS. However, both the effective masses are larger in ZnS than in CdSe, and this lowers the effective kinetic energies for that part of the wave function that extends into the ZnS core. The first effect tends to shift the state to higher energy (quantum confinement) while the second effect tends to shift it to lower energy, with increasing ZnS diameter. The net shift of the 1S-1S state to higher energy *is not monotonic* in Figure 10. Very small 5 and 10 Å ZnS inclusions *stabilize* the excited state by some 20 nm. ZnS inclusions of 15 to 30 Å show a net blue shift, and a decreasing transition intensity.

The calculation indicates that a distribution of 15 Å and smaller ZnS inclusions will effectively *inhomogeneously broaden* the transition, by inducing small shifts to higher and lower energies. This is the effect seen in Figure 4 for $(ZnS)_1(CdSe)_4Ph$ particles. This broadening is not removed by annealing. Quite likely there is additional broadening due to the position of the inclusion as well.

V. Discussion and Summary

Synthesis of 35–40 Å diameter (CdSe)Ph crystallites at 23 °C in inverse micelle solution produces internally polycrystalline particles whose X-ray coherence length is about one-third of the diameter. Annealing at 169 °C creates a near single crystal particle as judged by X-ray scattering and markedly narrows the 1S–1S optical transition. Bulk CdSe melts at 1512 K and anneals at a temperature much higher than 169 °C. Small particles would be expected to anneal at lower temperatures than bulk materal because of the free surface.

A 45 Å diameter, polycrystalline CdSe particle anneals *coherently* on a tiny internal ZnS fragment at 169 °C. The CdSe X-ray coherence length extends across the entire particle, and the composite particles show TEM lattice fringes. The particles show a greater 1S–1S absorption width, and much weaker fluorescence, than genuine CdSe particles. EDS measurements set an upper limit of about 18 Å for the ZnS seed. Theoretical modeling of the absorption spectrum sets an upper limit of about 15 Å. The ZnS seeds appear to be etched from an initial 25-Å size by reaction 2, and the interface is probably not abrupt. The data are consistent with either layered growth on an interior ZnS core or composite growth on a ZnS seed that remains at or near the surface.

Analysis of the Debye equation indicates that crystalline powder X-ray scattering is essentially blind to the presence of a small foreign inclusion. Analysis of the electronic structure shows that the lowest excited state energy and oscillator strength are also remarkably insensitive to the presence of a small inclusion. Only small shifts to either higher or lower energy occur, depending on size, band offsets, and effective masses. Composite particle luminescence is quite sensitive to deep traps causing nonradiative recombination, if such defects are introduced by the foreign inclusion.

Under present conditions, ZnS grows on a CdSe seed only to an effective thickness of about 4 Å. This surface layer prevents 169 °C annealing of the CdSe core and does not alloy with the CdSe core. These observations are consistent with the lower solid state mobility of Zn and S in ZnS than of Cd and Se in CdSe, as indicated by their respective melting points. Surface ZnS also changes surface deep trap luminescence into edge luminescence, reflecting a strong bonding of ZnS to CdSe. This particular observation indicates that the surface ZnS layer must be fairly uniform around the CdSe core. However, the surface ZnS layer is not coherent around the particle, as judged by the absence of the sharp line X-ray scattering expected for a coherent thin shell (Figure 8).

Comparison of the four different particles involving CdSe indicates (a) edge luminescence is not correlated with the presence of a single-crystal X-ray scattering, and (b) surface ZnS, but not interior ZnS or surface organic ligands, prevents low-temperature CdSe annealing.

We have clearly demonstrated nucleation, and partial growth, of composite semiconductor particles despite the fact that the two materials have bond lengths differing by 13%. However, organized growth, with the crystal lattice of one material having a definite structural relationship to that of the other material, is not observed under our conditions. It would be interesting to extend these studies to materials having a closer match in lattice (i.e., bond length). In changing materials, one also changes electronic structures. ZnSe and CdS have similar band gaps and a lattice mismatch of only 2.5%. Nevertheless, there is a significant offset in the absolute energies of the valence bands. This combination of properties should cause an interesting electronic structure, and studies of composite particles made from these materials are presently underway.

Acknowledgment. We thank a referee for suggesting the importance of reaction 2. We also thank A. Lovinger and F. Padden for the use of electron microscope facilities.

(21) Brus, L. E. *J. Chem. Phys.* **1984**, *80*, 4403.